Molecular Dynamics Study of Polarity in Room-Temperature Ionic Liquids

Vasiliy Znamenskiy[†] and Mark N. Kobrak*

Department of Chemistry, Brooklyn College and the Graduate Center of the City University of New York, 2900 Bedford Avenue, Brooklyn, New York 11210

Received: July 1, 2003; In Final Form: October 5, 2003

In this work, we use molecular dynamics simulation to explore the physical principles governing the polarity of room-temperature ionic liquids. We use the calculated absorption spectrum of the solvatochromic dye molecule betaine-30 as a proxy for polarity and characterize the solute−solvent interactions responsible for the solvatochromic shift. We analyze specific solute−solvent interactions and discuss the complications posed by the proximity of counterions in solution. We also explore the question of competition between solute−solvent and solvent−solvent interactions and find evidence supporting a recently proposed scheme for control of solvent polarity. Finally, we show that nonspecific electrostatic solute−solvent interactions are screened by the ionic solvent, dictating that the thermodynamic properties of solvation are determined by local interactions. However, thermal fluctuations create transient long-ranged solute−solvent interactions that could be important for chemical kinetics.

I. Introduction

The past decade has seen an explosion of research devoted to the adoption of room-temperature molten salts as solvents for chemical processing. These salts, commonly referred to as ionic liquids (ILs), possess many useful properties in this application. They are nonflammable, display a wide liquidus temperature range, and possess the negligibly small vapor pressure characteristic of all ionic materials.[1,2] The last property makes ILs highly desirable as replacements for volatile organic solvents in industry, where they could eliminate the health and environmental costs associated with solvent emissions from chemical processing.[3,4] Experiments have already proven that ILs are capable of acting as solvents for an enormous range of synthetic,[5−10] separatory,[11−14] and electrochemical[15−19] processes. Little is known about the connection between an ionic liquid's solvation properties and its ionic structure, however, and a fundamental theory connecting the two would greatly aid researchers in the field.

Perhaps the most important quantity in the choice of a solvent is its polarity. In molecular liquids, polarity may be qualitatively understood by examination of the electrostatic dipole moment and hydrogen-bonding properties of individual solvent molecules. But by definition, ions possess a nonzero electrostatic monopole moment (charge) that should dominate dipolar and higher-order terms.[20] Furthermore, ion−ion interactions lead to considerable charge-ordering in molten salt systems,[21] producing a qualitatively different environment than the ensemble of interacting dipoles formed by a molecular liquid. The unique nature of the environment makes it unclear that conventional concepts such as that of a "solvation shell" should be applied to ionic liquids, and the highly structured nature of ILs makes the utility of continuum models for the solvent suspect. Understanding polarity in ILs therefore requires a careful rethinking of the fundamental nature of solvation, and must begin with explicit simulation of solute−solvent interactions.

To date, there have been relatively few simulation studies of IL systems,[22−29] and most of these have centered on the structural, transport, and thermodynamic properties of ILs. Lynden-Bell and co-workers[27,28] have performed molecular dynamics simulations on a series of small molecules of varying polarity interacting with a model imidazolium chloride IL and calculated excess chemical potentials for each.[28] Their analysis of structural and energetic factors influencing the solute−solvent interaction indicates that, where applicable, hydrogen-bonding interactions between the solute and the chloride anion are the greatest influence on the solute−solvent interaction. However, though their analysis is intriguing, it does not provide a clear picture of how specific and nonspecific interactions affect the overall polarity of the ionic solvent. A more detailed decomposition of solute−solvent interactions is necessary for this, requiring a theoretically accessible proxy for polarity.

In this work, we use molecular dynamics simulation to study the nature of solvent polarity in an IL system. We calculate the absorption spectrum of the solvatochromic probe molecule betaine-30 in an IL solvent and characterize the solute−solvent interactions responsible for the solvatochromic shift. This spectroscopic shift is a well-known indicator for polarity,[30] and the solute−solvent interactions responsible for it can be analyzed in simulation. Our results indicate that specific solute−solvent interactions possess a character similar to those in molecular solvents but are complicated by the presence of solvent counterions. We also find evidence supporting a proposal by Crowhurst et al.[31] that polarity can be controlled by creating solvent−solvent interactions that compete with specific solute−solvent interactions. Finally, we observe that electrostatic screening by the solvent gives nonspecific electrostatic interactions a short-ranged character in the thermodynamic limit, but fluctuations in solvent configuration lead to long-ranged interactions that could be of kinetic importance.

* Corresponding author. E-mail: mkobrak@brooklyn.cuny.edu.
[†] Current address: Department of Chemistry, Marshak Science Building J-1024, City College of the New York - CUNY, Convent Ave & 138th St., New York, NY 10031.

10.1021/jp035891m CCC: $27.50
Published on Web 12/18/2003

II. Background

A. Molten Salts. It is instructive to begin by considering high-temperature molten salts, such as alkali halides. Neutron diffraction[32] and X-ray diffraction[33] studies on alkali halides have shown that though coordination numbers decrease on melting, cation−anion distances typically decrease. This indicates that fused salts retain much of the order of the solid-state lattice on melting, an observation supported by atomistic simulations of molten salts.[21,34,35] The resultant picture is strongly reminiscent of an ordered lattice with a large number of vacancies,[36,37] a configuration that can be understood by considering that the free energy of the system should be minimized by the creation of an approximately uniform distribution of charge. Insertion of a molecular solute into a fused salt necessarily interrupts the charge distribution, and the solvation process therefore represents a competition between the need to minimize the energy of solute−solvent interactions (dipole−ion) and solvent−solvent (ion−ion) interactions. The outcome of this competition determines the solvent polarity.

B. Nature of Polarity. Analysis of the polarity of a liquid is complicated by the lack of a rigorous theoretical definition for polarity.[30] Early discussions of polarity often restricted the term to nonspecific electrostatic interactions between solute and solvent,[30] but the importance of specific interactions such as hydrogen-bonding to solvation behavior has led to an expansion of the definition to include all specific and nonspecific interactions between solute and solvent species.[30,38] Although the theoretical investigation of simple model solutes might permit analysis of nonspecific interactions, or well-defined specific ones, it would be difficult to interpret such results without some understanding of the relative importance of specific and nonspecific interactions in IL solvents. This study makes use of a detailed physical model for one solute species, facilitating a comparison of specific and nonspecific interactions in ILs that can be used as a reference when more simple models are analyzed.

The characterization of polarity is always empirical, and scales of polarity are typically based on one of two types of experiments. The first involves the partitioning of a series of probe molecules of different character between the unknown phase and a phase of known polarity. A number of experiments of this type have been conducted on ionic liquids, including partitioning in a water−IL bilayer[39,40] and gas-phase chromatography,[41,42] in which the IL phase is used as a stationary phase and eluents act as probe molecules. The overall trend in these experiments seems to indicate that ILs behave as a moderately polar organic solvent.

A second approach makes use of solvatochromism, the shift in the optical absorption or emission spectrum of a chromophore in response to its chemical environment. This is a well-established tool for the study of solvent polarity,[30] and studies of various chromophores in ionic liquids[43−50] seem consistent with the description obtained from the partitioning studies given above (though some ambiguities exist[50]). We choose solvatochromism as a proxy for polarity in our simulations, as modeling the partitioning of solute species between solvents requires computationally intensive calculation of their relative free energies of solvation.[51] Although accurate simulation of optical processes in solution requires explicit inclusion of the electronic degrees of freedom for the chromophore,[52−54] previous studies[55−57] have shown that relatively simple calculations can yield considerable insight on the solute−solvent interactions responsible for solvatochromism.

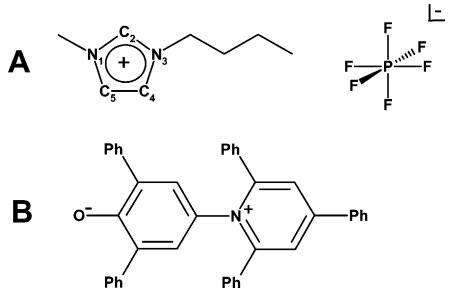

Figure 1. (A) 1-Butyl-3-methylimidazolium hexafluorophosphate (BMIM[PF_6]). (B) Betaine-30. Ph- denotes a phenyl group.

We choose to simulate the photoexcitation of betaine-30 in 1-butyl-3-methylimidazolium hexafluorophosphate (BMIM-[PF_6]), shown in Figure 1. The choice is motivated by the existence of previous theoretical studies on betaine-30,[52−54,56] and the availability of experimental data on its behavior in various ILs.[43−47] The use of betaine-30 allows consideration of both nonspecific and specific interactions, as the solvatochromic shift of betaine-30 is known to be sensitive to the hydrogen-bonding character of the solvent.[30] We obtain an estimated absorption spectrum using molecular dynamics simulation, and characterize the microscopic solute−solvent interactions responsible for the observed solvatochromic shift.

III. Methodology

A. Polarity from Simulation Data. Mente and Maroncelli[56] have shown that it is possible to reproduce the solvatochromic shift of betaine-30 based on calculations of electronic structure performed on the isolated chromophore. In this model, the difference between ground and excited electronic states of the betaine-30 molecule is accounted for entirely in the charge configuration of the chromophore, such that excitation consists of a redistribution of charge between atomic sites with no change to chromophore geometry or dispersive interactions.

We define the quantity Z to be the difference in excitation energy between the solvated chromophore and the isolated chromophore, such that

$$Z = (V_e^s(\mathbf{r},\mathbf{R}) - V_g^s(\mathbf{r},\mathbf{R})) - (V_e^o(\mathbf{r}) - V_g^o(\mathbf{r})) \qquad (1)$$

$V_g^o(\boldsymbol{r})$ and $V_e^o(\boldsymbol{r})$ denote the ground and excited electronic energies of the isolated chromophore, $V_g^s(\mathbf{r},\mathbf{R})$ and $V_e^s(\mathbf{r},\mathbf{R})$ denote the corresponding energies for the chromophore in the solvent environment, and the vectors $\mathbf{r}$ and $\mathbf{R}$ contain the coordinates of the solute and solvent atomic sites, respectively. Calculation of the absorption spectrum requires knowledge of the distribution of Z for the solvent at equilibrium with the ground-state charge distribution of the chromophore. The absorption spectrum is then approximated by a histogram in the difference between ground and excited-state energies in solution ΔE_s,

$$\begin{aligned}\Delta E_s &= V_e^s(\mathbf{r},\mathbf{R}) - V_g^s(\mathbf{r},\mathbf{R}) \\ &= (V_e^o(\mathbf{r}) - V_g^o(\mathbf{r})) + Z \end{aligned} \qquad (2)$$

In our calculation of the absorption spectrum, we follow the example of Mente and Maroncelli[56] and use an experimentally obtained value of 30.7 kcal/mol[30] for the excitation energy of the isolated chromophore ($V_e^o(\mathbf{r}) - V_g^o(\mathbf{r})$). This represents the excitation energy of betaine-30 in the nonpolarizable liquid tetramethylsilane, as experimental difficulties prevent measurements on the chromophore in the gas phase.

It will be useful in subsequent discussion to break Z down into components Z_i, which correspond to the contribution to Z from the ith ion. This yields

$$Z = \sum_{i}^{N} Z_i \tag{3}$$

where N is the total number of ions in the system. As indicated above, solute−solvent dispersive interactions are unchanged in this model of the photoexcitation process, and the values Z_i depend only on Coulomb interactions

$$Z_i = \sum_{j}^{n_c}\sum_{k}^{n_i}\left(\frac{q_j^{c,e} q_k^i}{R_{i,jk}}\right) - \left(\frac{q_j^{c,g} q_k^i}{R_{i,jk}}\right)$$

$$= \sum_{j}^{n_c}\sum_{k}^{n_i}\left(\frac{\Delta q_j^c q_k^i}{R_{i,jk}}\right) \tag{4}$$

where $R_{i,jk}$ denotes the distance between the jth site on the chromophore and the kth site on the ith solvent ion, and n_c and n_i denote the number of sites in the chromophore and solvent ion, respectively. The value q_k^i indicates the charge of the kth site on the ith solvent ion, and $q_j^{c,x}$ denotes the charge on the jth site on the chromophore in the x electronic state. Finally, $\Delta q_j^c = q_j^{c,e} - q_j^{c,g}$.

Z represents the difference in the solute−solvent electrostatic interaction energies for the ground and excited chromophore states. The ensemble average of Z is the negative of the solvatochromic shift, and the link between solvatochromism and polarity makes Z a numerical estimator for solvent polarity. We note for completeness that Z is in fact the solvent coordinate for Marcus theory,[58] and the simulations carried out here are analogous to a Sumi−Marcus treatment of photoexcitation.[59]

B. Simulation. We use the force field of Shah et al.[24] to treat the BMIM[PF_6] system. This force field is based on the optimized potentials for liquid simulations (OPLS) parametrization,[60] with a united atom treatment of CH_n groups. The imidazolium ring and its methyl substituent are treated as rigid bodies using the quaternion method,[61] whereas the butyl substituent is allowed torsional, angular bending, and bond stretching degrees of freedom. The angular and stretching components of the butyl motion are not included in the Shah et al. Monte Carlo study, and force constants for these motions were adopted from intramolecular potentials of the AMBER[62] force field. The simulation was carried out under cubic periodic boundary conditions, with Coulomb interactions treated via the Ewald summation.[61]

The time step for molecular dynamics was set at 0.5 fs, with convergence verified by back-integration in an NVE ensemble. All reported data were collected in an isothermal, isobaric ensemble at 300 K and 1 atm, using a Nosé−Hoover thermostat[63,64] and an Anderson barostat.[65] Time constants for the thermostat and barostat were $\tau_T = 0.5$ ps and $\tau_P = 2.0$ ps, respectively, with the functional forms of the integration algorithms presented in eqs 2.181 and 2.190 of ref 66. Equilibration was accomplished in two stages, beginning with a propagation in an NVE ensemble to eliminate bad contacts associated with the random initial configuration. This was followed by roughly 1000 ps of equilibration time in the NPT ensemble. Consistency with the Shah et al.[24] The Monte Carlo study was verified by simulation of the neat liquid and reproduction of the previously computed density.[24] The value

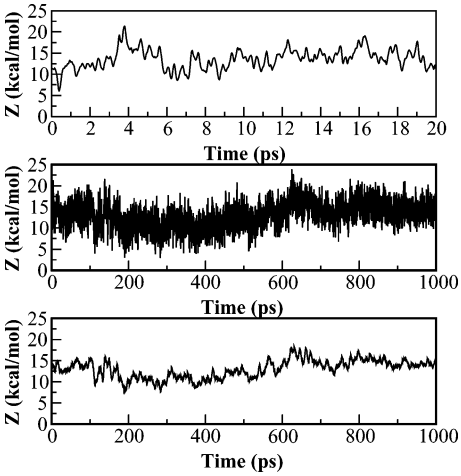

Figure 2. (Top) Z vs time for a sample trajectory. (Middle) Z vs time for the same trajectory, followed for 1 ns. (Bottom) same trajectory, with Z averaged over 5 ps intervals to eliminate the subpicosecond component of the motion.

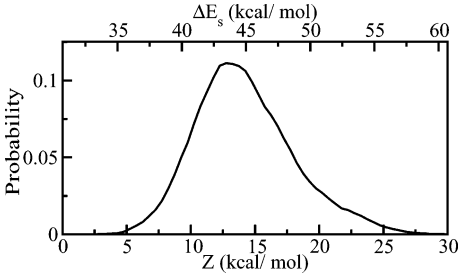

Figure 3. Statistical distribution in Z over all time, all trajectories. Bottom x-axis shows the value of Z, top x-axis shows the corresponding excitation energy ΔE_s.

observed in the present simulations was 1.95×10^{-4} m^3/mol at 300 K, compared to 2.01×10^{-4} m^3/mol at 298 K in the previous study. The difference is likely due to the inclusion of the additional internal vibrational modes identified above, as previous studies have shown that IL density may be sensitive to the treatment of the side-chain.[25]

Our parameters for the betaine-30 chromophore are based on the OPLS model, as implemented by Mente and Maroncelli.[56] As discussed in section III.A, photoexcitation is taken to consist purely of a redistribution of electrostatic charge among the chromophore sites. The sign and magnitude of the change in the electrostatic charge on each chromophore site is indicated graphically in Figure 3 of ref 56; photoexcitation consists mainly of a flow of electron charge density away from the oxygen to the nitrogen and its neighboring carbons. As in the Mente and Maroncelli study, the chromophore is held rigid throughout the calculation. Because our interest is in observing only the motion of the solvent, we also eliminate chromophore rotational and translational motion. This technique has been used previously in electron-transfer calculations where interpretation of solvent behavior is the sole objective of the simulation[67,68] and does not significantly affect the equilibrium energetics for the system. Formally, this makes the coordinate vector $\mathbf{r}$ defined in section III.A a constant.

The simulations of the betaine-30 spectrum reported here consist of a single chromophore interacting with 200 IL solvent ion pairs. Convergence in the Z distribution with respect to the number of solvent ions was verified by comparison to simulations of betaine-30 interacting with 108 ion pairs. Our study of solvatochromism made use of twelve trajectories, each brought to equilibrium and integrated in time for one nanosecond.

IV. Results and Discussion

A. Calculation of the Absorption Spectrum. The values of Z obtained from a sample trajectory are shown in Figure 2. The trajectory exhibits motion on two time scales, one subpicosecond and the other on the order of hundreds of picoseconds. The latter is most easily visible when the value of Z is averaged over 5 ps intervals to eliminate the effect of subpicosecond motion. This is consistent with the results of time-resolved fluorescence spectroscopy in ILs,[69,70] where a similar separation of time scales is inferred. A more detailed analysis of the dynamics will be the subject of future work. The Z values resulting from the 12 trajectories can be sorted into a histogram and used to calculate an absorption spectrum, as indicated by eq 2. Figure 3 shows the resultant histogram and the calculated absorption spectrum.

The peak in the calculated absorption spectrum occurs at a shift of 12.7 kcal/mol relative to the isolated chromophore, whereas the experimental peak occurs at 21.6 kcal/mol. This represents a 41% error, significantly larger than the average errors observed by Mente and Maroncelli in their study of betaine-30 in molecular liquids. Much of the error likely arises from the use of a first-generation force field for the IL, which lacks the refinement of force fields for better understood molecular solvents. But it is also worth considering that the interaction between the solute and individual solvent ions is stronger in ILs than in molecular liquids, owing to the character of ion−dipole interactions. This certainly complicates the specific interactions discussed in section IV.B and could make the calculation more sensitive to small errors in the force field. Finally, we note that neither the force field described in section III.B nor those used by Mente and Maroncelli account for the electronic polarizability of solvent species. Some properties of fused salt systems are known to be sensitive to ionic polarizability,[35] and despite some indications to the contrary[71] it is possible that this property may be more important to IL behavior than to molecular liquids. Regardless of these quantitative issues, the analysis presented here provides qualitative insight into the solute−solvent interactions responsible for the observed polarity of IL solvents.

B. Specific Solute−Solvent Interactions. It is well-known that specific solute−solvent interactions involving the oxygen atom of betaine-30 are important determinants of the solvatochromic shift.[30] We therefore consider the radial distribution functions (RDFs) of solvent ions about the solute oxygen, shown in Figure 4. Examination of the radial number for BMIM shows that the solute oxygen has one well-defined nearest neighbor, and the sharp peak in the BMIM RDF indicates a strong association. The nature of the interaction is clearer when the BMIM is decomposed into a center-of-mass for the butyl group, and a center of mass for the ring system and methyl group. The positively charged ring of the BMIM is on average closer than the tail, as one would expect from simple Coulomb arguments. The overlap of the RDFs for the ring and tail indicates some rotation, and the double-peaked structure of the O-ring distribution indicates the existence of multiple configurations for the cation (discussed below). Comparing this to the RDF for the PF_6^- ion, one observes that the nearest anion is slightly further away from the oxygen, its position determined by its attraction to the BMIM and its repulsion from the oxygen.

Imidazolium-based ionic liquids have been shown experimentally to be hydrogen bond donors,[72] and though the extent of H-bonding to specific anionic species has been the subject of debate,[73,74] it can reasonably be expected that the C_2 carbon of the imidazolium ring (see Figure 1) will associate with a good H-bond acceptor such as the betaine oxygen. Hydrogen-bonding between the solute oxygen and the solvent is an important determinant of solvatochromic shift in betaine-30, and Mente and Maroncelli gained considerable insight into solute−solvent interactions by examining hydrogen-bonding to the chromophore oxygen. However, because the OPLS treatment of intermolecular interactions incorporates H-bonding into Coulomb interactions, it is impossible to quantify the energetics of hydrogen-bonding directly from simulations of this type. Mente and Maroncelli[56] circumvented this difficulty by calculating the total solvatochromic shift arising from the chromophore's interaction with the solvent molecule nearest to the oxygen. We proceed in the same vein.

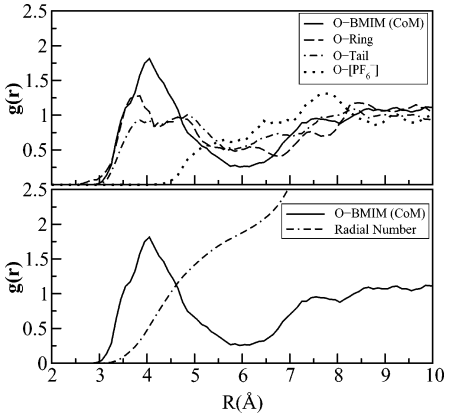

Figure 4. (Top) radial distribution function of solvent ions and its components about the solute oxygen, as described in the text. In the legend, "CoM" denotes the center of mass for the complete BMIM ion, and Tail and Head denote the centers of mass for the butyl group and the ring (including methyl group) substituents, respectively. (Bottom) comparison of BMIM CoM radial distribution function described above with radial number, the average population of BMIM ions as a function of distance from the oxygen center. Note that the radial number is equal to 1 at a distance of 4.5 Å, implying that the first peak in the RDF corresponds almost entirely to a single BMIM.

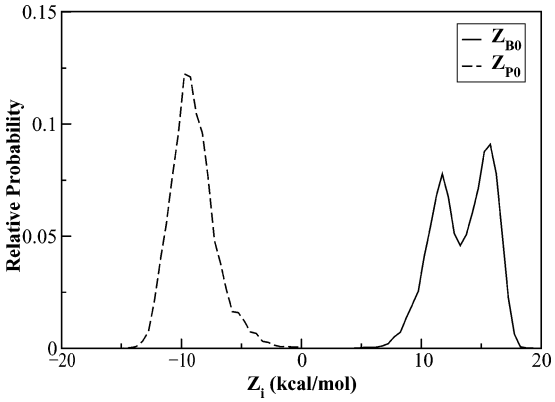

Figure 5. Distribution in Z_i for the BMIM ion and PF_6 ion most closely associated with the solute oxygen, as described in the text.

We define R_{C-O} to be the distance from the betaine oxygen to the C_2 site of the nearest BMIM, and select the nearest cation on the basis of this distance. We indicate the value of Z_i for this ion as Z_{B0}, with Z_i defined in section III.A. We likewise identify the nearest anion on the basis of the oxygen-phosphorus distance, and define its contribution to Z as Z_{P0}. Figure 5 shows the ensemble distribution of of these values. The most obvious point is that where the average Z_{B0} is 13.5 kcal/mol, the value of Z_{P0} is −9.0 kcal/mol, largely canceling the effect of the proximal BMIM. Although these two ions possess particularly large values of Z_i, the charge-ordering of the solvent dictates

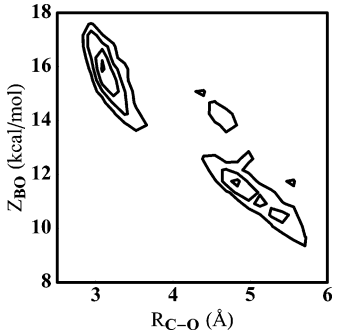

Figure 6. Contour plot showing the ensemble probability density in Z_{BO} and R_{C-O}, as described in the text.

that the pattern of near-cancellation by counterions must repeat throughout the solvent. This phenomenon contrasts with the results of Mente and Maroncelli,[56] who observed that the contribution of the nearest solvent molecule was always a relatively small fraction of the total solvatochromic shift.

It is informative to consider the double-peaked character of the Z_{B0} distribution in Figure 5. This bifurcation can be interpreted with the aid of Figure 6, which shows the ensemble probability distribution in Z_{B0} and R_{C-O}. It is clear that the BMIM exists primarily in two configurations relative to the betaine oxygen, one configuration in which the C_2 carbon is roughly 3.1 Å from the betaine oxygen, and one in which it is 5−6 Å away; the two regions have different characteristic distributions in Z_{B0}, leading to the double-peaked structure in Figure 5. These configurations can be interpreted with the aid of Figure 4: The double-peaked structure in the ring-oxygen RDF likely arises from the existence of two configurations, but the single peak in the BMIM center of mass distribution indicates the difference between the two states is primarily orientational rather than translational.

The distance of 3.1 Å is characteristic of C_2−O hydrogen bonding, as expected on the basis of the arguments above. The 5 kcal/mol shift in Z associated with the creation or destruction of the H-bond is comparable to the shifts associated with H-bonding in Mente and Maroncelli's simulations (see Figure 9 of ref 56), though in the present case some of the shift may arise from Coulombic interactions between the solute and charged sites on the imidazolium ring other than C_2. The spontaneous breaking of the H-bond at thermal energies indicates that it is relatively weak, a result that would explain the fact that Lynden-Bell and co-workers did not observe significant energetic effects due to BMIM C_2-site H-bonding to molecular solutes in their solvation simulations.[28]

Analysis of solvent−solvent interactions provides context for understanding the two features in Figure 6. In their presentation of the force field used in this study, Shah et al.[24] observed that the anion associated most strongly with the C_2 carbon and with the C_4 and C_5 carbons. This seems to be the case for the oxygen, with the peak at $R_{C-O} = 3.1$ Å corresponding to the former and at ∼5 Å corresponding to the latter. It is unclear whether the C_2 site H-bonds to PF_6^-, and though the creators of the force field note strong C_2−PF_6^- interactions, they do not address the question of H-bonding explicitly.[24] Regardless, the double-peaked structure of Figure 6 indicates an equilibrium between states in which the C_2-site is associated with the solute, and states in which it is associated with the solvent anion.

Sample configurations of the C_2 carbon in association with the solute and the anion are given in Figure 7. In the configuration shown in (A) and (B), the distance and orientation of the BMIM ion seem consistent with a C_2−O H-bond. The

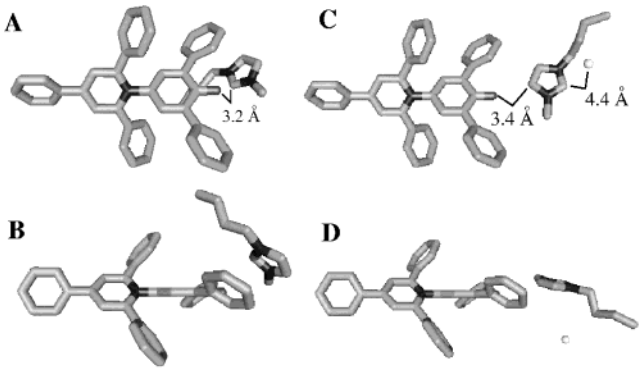

Figure 7. (A) Sample configuration of betaine-30 and nearest BMIM, with the C_2 carbon oriented toward the betaine oxygen. (B) Same configuration, rotated 90°. (C) Sample configuration of betaine-30 and nearest BMIM and PF_6. Here, the C_5 carbon is oriented to the oxygen, and the C_2 carbon is associated with the anion. (D) Same configuration, rotated 90°.

association of the imidazolium ring with the nearby betaine phenyl ring seems consistent with previous studies of π-stacking in ionic liquids,[29] though we do not explore this question in detail. The configuration shown in parts C and D of Figure 7 show a close association between the solute oxygen and the BMIM C_5-site, and an association between the C_2 site and the nearest PF_6. The united atom treatment of the anion dictates that the measured distance of 4.4 Å corresponds to a distance from the C_2-site to the anion phosphorus, and therefore provides no insight into the question of whether this represents hydrogen-bonding. Thus, though UA treatments often provide good agreement with all-atom models,[75] we do not believe a deeper investigation of cation−anion hydrogen bonding within this model would be fruitful.

Despite the questions regarding the character of C_2-anion interactions for this system, the observation of an equilibrium between solute−solvent and solvent−solvent interactions has important implications for solvent polarity. PF_6^- is a weak nucleophile, and replacing it with a more H-bond labile species could increase the degree of C_2 association with the anion. This would decrease the average value of Z and therefore reduce the effective solvent polarity. Crowhurst et al.[31] recently argued for the existence of such a competition on the basis of experimental evidence, and our results support their interpretation. Thus, although the use of more H-bond labile anions may lead to experimental complications (e.g., elevation of solvent melting point), the creation of competitive solvent−solvent interactions as a means of decreasing the strength of solute−solvent interactions could be a potentially valuable mechanism for the control of solvent polarity.

C. Nonspecific Solute−Solvent Interactions. We now consider nonspecific electrostatic interactions between the solute and the solvent. We begin by characterizing the spatial distribution of ions that most strongly affect the solvatochromic shift (i.e., have the largest $|Z_i|$). This distribution is shown in Figure 8. The projection of the three-dimensional figure into two dimensions loses some information, but it is clear that the most strongly contributing ions are distributed in a dumbbell shape about the solute dipole. This is to be expected from simple electrostatic arguments, as an ion near the dipole's geometric center is equidistant from both charges and so has no net energetic interaction with the dipole.

This would seem to invalidate the concept of a "solvent shell" in ionic liquids, as solvent contribution to polarity does not index directly with solute−solvent distance even on average. Yet a more detailed examination reveals that the concept of a solvation

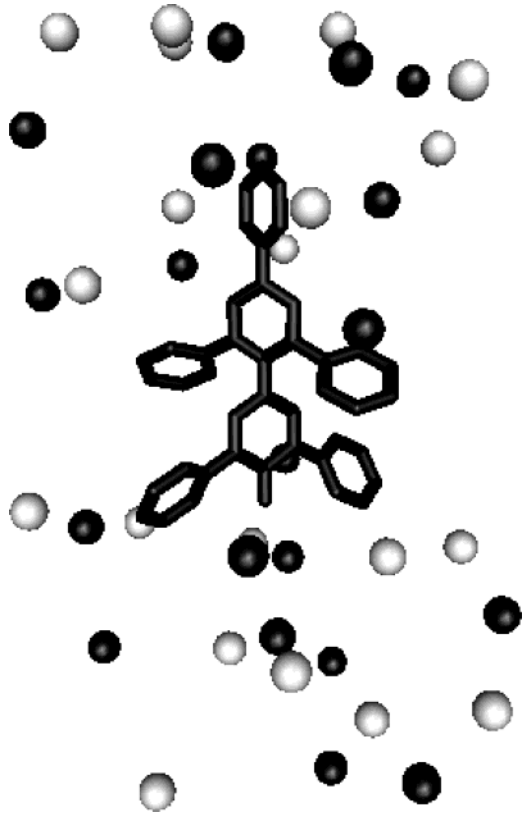

Figure 8. Centers of mass for the forty ions displaying the largest $|Z_i|$, as described in the text. Spheres indicate centers of mass; cations are indicated with light shading, and anions are indicated by dark shading. The position of the chromophore is given by the stick diagram.

shell still applies. This can be shown through calculation of the contribution of ions to the value of Z as a function of their distance $\mathscr{R}$ from the chromophore. To this end, we define the function

$$\zeta(\mathscr{R}) = \sum_{i}^{N} Z_i \Theta(\mathscr{R}_i - \mathscr{R}, \Delta) \tag{5}$$

where

$$\Theta(x,\Delta) = 1 \qquad |x| \le \frac{\Delta}{2}$$

$$= 0 \qquad |x| > \frac{\Delta}{2} \tag{6}$$

Z_i is defined in eq 4 and $\mathscr{R}_i$ is defined to be the shortest distance from any site on the chromophore to any site on the ith solvent ion. In this work, Δ is taken to be 0.2 Å. Note that

$$Z = \frac{1}{\Delta}\int_0^\infty d\mathscr{R}\, \zeta(\mathscr{R}) \tag{7}$$

Plots of $\zeta(\mathscr{R})$ for several trajectories and averaged over all data are shown in Figure 9. Parts A−D of Figure 9 show relatively short-time averages of the contribution to Z by solvent ions at a given solute−solvent distance $\mathscr{R}$. The significant differences between these four plots indicate that fluctuations in solvent configuration can strongly influence the contribution to Z by different solvent layers. Their persistence on 100 ps time scales suggests these fluctuations are long-lived and result from some form of collective solvent vibrational motion. These fluctuations presumably influence local charge densities and create transient

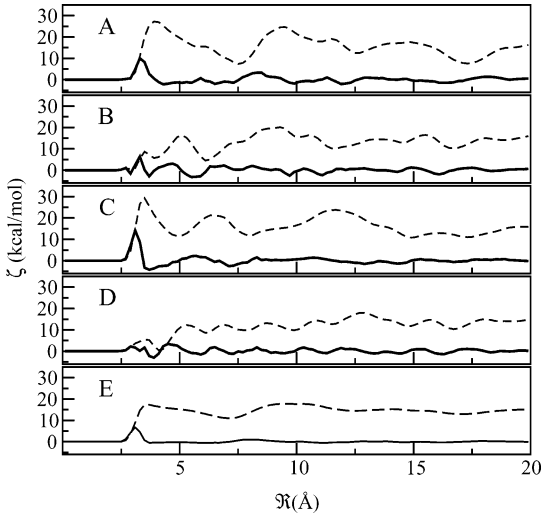

Figure 9. (A)−(D) Solid line: $\zeta(\mathscr{R})$ for four trajectories. Dashed line: $\int d\mathscr{R}\, \zeta(\mathscr{R})$, the integrated contribution to Z as a function of distance. Each figure shows a different sample trajectory, averaged over 100 ps of data. (E) Contribution to Z by solvent ions a distance $\mathscr{R}$ from the chromophore, averaged over all time for all trajectories.

electrostatic dipole moments that interact strongly with the chromophore. The existence of such long-period collective motions is consistent with experimental data, as terahertz spectroscopic studies of ILs similar to BMIM[PF_6][76,77] have indicated the existence of dipole-active solvent motions with time scales ranging from <30 fs to roughly 1 ns.

However, part E of Figure 9 indicates that the ensemble average of Z vs $\mathscr{R}$ shows relatively little variation after the first two layers of solvent. Beyond this point, the solvent assumes the configuration of the bulk liquid and therefore creates a nearly uniform charge distribution. Some residual fluctuations in Z vs $\mathscr{R}$ remain due to the charge-ordering of fused salts, which persists on length scales comparable to multiple unit cells of the solid-state structure,[21] but the medium does not on average affect the value of Z.

At first glance, this situation seems paradoxical. The fluctuations observed in parts A−D of Figure 9 imply the existence of collective solvent vibrational modes with a nonzero electrostatic dipole moment, that interact with the chromophore. The fact that these modes spontaneously fluctuate at thermal energies indicates that they are not excessively rigid. This implies that the presence of the chromophore's permanent dipole should shift the equilibrium position of those modes, creating a nonzero solute−solvent interaction (i.e., polarizing the medium). But the fact that Z does not rise significantly after the second solvation shell indicates that the medium is unpolarized.

The paradox can be resolved by consideration of the electrostatic screening behavior of a fused salt.[78] In the thermodynamic limit, external electric fields (such as that of a chromophore) are screened by the closest layers of the fused salt, so that the electric field cancels within the bulk material. Thus, the net interaction with distant collective motions of the solvent is zero and the solvent is unpolarized. This is analogous to the cancellation of an electric field at the surface of a conductor.[20] The fluctuations in ζ vs $\mathscr{R}$ observed on finite time scales are explained by the fact that charge density must fluctuate as a function of time, as does any observable in an ensemble.[79] Screening is a thermodynamic property, so fluctuations in charge density (either among distant ions or among the ions responsible for screening) will lead to transient nonzero solute−solvent interactions. Thus, though individual long-ranged

ion−dipole interactions are strong, screening effects lead to nonspecific interactions with a local character and the concept of a solvation shell can be applied in ILs.

One should be able to characterize the nature of electrostatic screening in ILs by examination of the local solvent structure about the solute. We have not yet done so in a detailed way, but some insight can be gleaned by examination of Figure 9E. The rapid rise in Z at 3 Å occurs on contact with the nearest solvent ions, which interact favorably with the chromophore. The slow decrease in Z between 4 and 7 Å arises from the presence of counterions to those nearest neighbors, and the breadth of this feature indicates a broad distribution in the positions of these counterions. This could be expected from the slow rise in the radial distribution function between the betaine oxygen and the PF_6^- ion shown in Figure 4. These observations imply that specific solute−solvent interactions fix the position of the nearest ions, but their counterions are capable of adopting a large number of nearly degenerate configurations. How this freedom of motion affects screening or thermal fluctuations in effective polarity is unclear but any future analysis of screening must account for these differing behaviors.

V. Conclusion

The nature of solvation in ionic liquids is complex, and it would be absurd to expect it to be completely understood from a single study. However, the results presented here provide a framework for the analysis of future work. The process of hydrogen-bonding in molecular and ionic solvents is mechanically similar, in that the identity of the donor (the C_2 site of the imidazolium ion) and acceptor (the betaine-30 oxygen) is exactly as one would expect in conventional systems. But the presence of proximal counterions complicates analysis of specific interactions, because the net solute−solvent interaction must be much weaker than the magnitude of the individual interactions. The ability to vary the identity of the cation and anion creates unique opportunities for control of solvent−solvent interactions, allowing the creation of competition between solute−solvent and solvent−solvent interactions predicted by Crowhurst et al.[31] It is possible that this chemical variability may be exploited in other ways, creating still more novel avenues for control over the ionic liquid's chemical environment.

The potential for control of IL polarity through specific interactions is supported by our analysis of nonspecific interactions. We have demonstrated that electrostatic screening localizes nonspecific electrostatic contributions to polarity, and because minor chemical derivitizations of ion centers seem unlikely to affect this screening, changes in solvent polarity as a function of ionic structure can be understood by consideration solely of specific solute−solvent interactions. This is consistent with experiments.[43] However, the local character of nonspecific interactions applies only in the thermodynamic limit, and fluctuations in charge density at long range lead to transient contributions to solute−solvent electrostatic interactions. This effectively reduces the Gibbs free energy for motion along the polarization coordinate Z, and could be important in understanding kinetics in ionic liquids for processes involving polar transition states.[80] Solvation dynamics are central to understanding kinetic effects and will be the subject of future work.

Acknowledgment. We gratefully acknowledge Prof. Mark Maroncelli for providing information on the simulation of the betaine-30 chromophore, and Prof. Charles M. Gordon for providing access to the experimental spectrum of betaine-30 in BMIM[PF_6] observed in his laboratory. The molecular dynamics calculations reported here made use of modified computational routines from the DL_POLY 2.12 library developed by W. Smith and T. R. Forester at Daresbury Laboratory. This work was supported in part by a grant from the Professional Staff Congress of the City University of New York.

References and Notes

(1) Welton, T. *Chem. Rev.* **1999**, *99*, 2071−2083.
(2) Seddon. K. R. *J. Chem. Tech. Biotechnol.* **1997**, *68*, 351−356.
(3) Freemantle. M. *Chem. Eng. News* **2000**, *May 15 2000*, 37−50.
(4) Chauvin. Y.; Olivier-Bourbigou, H. *Chemtech* **1995**, *25*, 26−30.
(5) Dupont, J.; de Souza, R. F.; Suarez, P. A. Z. *Chem. Rev.* **2002**, *102*, 3667−3692.
(6) Jin, K.; Huang, X.; Pang, L.; Li, J.; Appel, A.; Wherland, S. *Chem. Commun.* **2002**, 2872−2873.
(7) Zhao, H.; Malhotra, S. V. *Aldrichim. Acta* **2002**, *35*, 75−83.
(8) Fischer, T.; Sethi, A.; Welton, T.; Woolf, J. *Telrahedron Lett.* **1999**, *40*, 793−796.
(9) Steines, S.; Wasserscheid, P.; Driessen-Hölscher, B. *J. Prakt. Chem.* **2000**, *342*, 348−354.
(10) Adams, C. J.; Earle, M. J.; Roberts, G.; Seddon, K. R. *Chem. Commun.* **1998**, 2097−2098.
(11) Swatloski, R. P.; Spear, S. K.; Holbrey, J. D.; Rogers, R. D. *J. Am. Chem. Soc.* **2002**, *124*, 4974−4975.
(12) Scurto, A. M.; Aki, S. N. V. K.; Brennecke, J. F. *J. Am. Chem. Soc.* **2002**, *124*, 10276−10277.
(13) Fadeev, A. G.; Meagher, M. M. *Chem. Commun.* **2001**, 205−206.
(14) Blanchard, L. A.; Hancu, D.; Beckman, E. J.; Brennecke, J. F. *Nature* **1999**, *399*, 28-29.
(15) Lagrost, C.; Carrié, D.; Vaultier, M.; Hapiot, P. *J. Phys. Chem. A* **2003**, *107*, 745−752.
(16) Katayama, Y.; Konishiike, I.; Miura, T.; Kishi, T. *J. Power Sources* **2002**, *109*, 327−332.
(17) Ryan, D. M.; Riechel, T. L.; Welton, T. *J. Electrochern. Soc.* **2002**, *149*, A371−A378.
(18) Wilkes, J. S.; Levisky, J. A.; Wilson, R. A.; Hussey, C. L. *Inorg. Chem.* **1982**, *21*, 1263−1264.
(19) Chum, H. L.; Koch, V. R.; Miller, L. L.; Oesteryoung, R. A. *J. Am. Chem. Soc.* **1975**, *97*, 3264−3265.
(20) Wangsness, R. K. *Electromagnetic Fields*, 2nd ed.; John Wiley & Sons: New York, 1986.
(21) Tosi, M. P.; Price, D. L.; Saboungi, M.-L. *Annu. Rev. Phys. Chem.* **1993**, *44*, 173−211.
(22) Margulis. C. J.; Stern, H. A.; Berne, B. *J. J. Phys. Chem. B* **2002**, *106*, 12017−12021.
(23) Morrow, T. 1.; Maginn, E. J. *J. Phys. Chem. B* **2002**, *106*, 12807−12813.
(24) Shah, J. K.; Brennecke, J. F.; Maginn, E. J. *Green Chem.* **2002**, *4*, 112−118.
(25) Hanke, C. C.; Price, S. L.; Lynden-Bell, R. M. *Mol. Phys.* **2001**, *99*, 801−809.
(26) de Andrade, J.; Böes, E. S.; Stassen, H. *J. Phys. Chem. B* **2002**, *106*, 3546−3548.
(27) Hanke, C. G.; Atamas, N. A.; Lynden-Bell, R. M. *Green Chem.* **2002**, *4*, 107−111.
(28) Lynden-Bell, R. M.; Atamas, N. A.; Vasilyuk, A.; Hanke, C. *G. Mol. Phys.* **2002**, *100*, 3225−3229.
(29) Hanke, C.; Johansson, A.; Harper, J.; Lynden-Bell, R. *Chem. Phys. Lett.* **2003**, *374*, 85−90.
(30) Reichardt, C. *Chem. Rev.* **1994**, *94*, 2319−2358.
(31) Crowhurst, L.; Mawdsley, P.; Perez-Arlandis, J.; Salter, P.; Welton, *T. Phys. Chem. Chem. Phys.* **2003**, *5*, 2790−2794.
(32) Levy, H. A.; Danford, M. D. Diffraction Studies of Molten Salts. In *Molten Salt Chemistry*; Blander, M., Ed.; Interscience Publishers: New York, 1964.
(33) Zarzycki, J. *J. Chem. Soc., Faraday Discuss.* **1961**, *32*, 38−48.
(34) Trullis, J.; Giró, A.; Padró, J. A.; Silbert, M. *Physica A* **1991**, *171*, 384−402.
(35) Rovere, M.; Tosi, M. P. *Rep. Prog. Phys.* **1986**, *49*, 1001−1081.
(36) Blander, M. Some Fundamental Concepts in the Chemistry of Molten Salts. In *Molten Salts: Characterization and Analysis*; Mamantov, G., Ed.; Marcel-Dekker: New York, 1969.
(37) Bloom, H.; Bockris, J. O. Structural Aspects of Ionic Liquids. In *Fused Salts*; Sundheim, B. R., Ed.; McGraw-Hill: New York, 1964.
(38) Miller, P. *Pure Appl. Chem.* **1994**, *66*, 1077.
(39) Abraham, M. H.; Zissimos, A. M.; Huddleston, J. G.; Willauer, H. D.; Rogers, R. D.; W. E. Acree, J. *Ind. Eng. Chem. Res.* **2003**, *42*, 413−418.
(40) Huddleston, J. G.; Willauer, H. D.; Swatloski, R. P.; Visser, A. E.; Rogers, R. D. *Chem. Commun.* **1998**, 1765−1766.

(41) Anderson, J. L.; Ding, J.; Welton, T.; Armstrong, D. W. *J. Am. Chem. Soc.* **2002**, *124*, 14247−14254.
(42) Armstrong, D. W.; He, L.; Liu, Y.-S. *Anal. Chem.* **1999**, *71*, 3873−3876.
(43) Dzyuba, S. V.; Bartsch, R. A. *Tetrahedron Lett.* **2002**, *43*, 4657−4659.
(44) Baker, S. N.; Baker, G. A.; Bright, F. V. *Green Chem.* **2002**, *4*, 165−169.
(45) Fletcher. K. A.; Pandey, S. *Appl. Spectrosc.* **2002**, *56*, 266−271.
(46) Muldoon, M. J.; Gordon, C. M.; Dunkin, I. R. *J. Chem. Soc., Perkin Trans.* **2001**, *2*, 433−435.
(47) Wasserscheid, P.; Gordon, C. M.; Hilgers, C.; Muldoon, M. J.; Dunkin, I. R. *Chem. Commun.* **2001**, 1186−1187.
(48) Aki, S. N. V. K.; Brennecke, J. F.; Samrnanta, A. *Chem. Commun.* **2001**, 413−414.
(49) Carmichael, A. J.; Seddon, K. R. *J. Phys. Org. Chem.* **2000**, *13*, 591−595.
(50) Borhôte, P.; Dias, A.-P.; Papageorgiou, N.; Kalyanasundaram, K.; Grätzel, M. *Inorg. Chem.* **1996**, *35*, 1168−1178.
(51) Kolhnlmanl, P. *Chem. Rev.* **1993**, *93*, 2395−2417.
(52) Lobaugh, J.; Rossky, P. J. *J. Phys. Chem. A* **2000**, *104*, 899−907.
(53) Lobaugh, J.; Rossky, P. J. *J. Phys. Chem. A* **1999**, *103*, 9432−9447.
(54) Walker, G. C.; Åkesson, E.; Johnson, A. E.; Levinger, N. E.; Barbara, P. F. *J. Phys. Chem.* **1992**, *96*, 3728−3736.
(55) Coutinho, K.; Saavedra, N.; Serrano, A.; Canuto, S. *J. Mol. Struct.* **2001**, *539*, 171−179.
(56) Mente, S. R.; Maroncelli, M. *J. Phys. Chem. B* **1999**, *103*, 7704−7719.
(57) DeBolt, S. E.; Kollman, P. *A. J. Am. Chem. Soc.* **1990**, *112*, 7515−7524.
(58) Marcus, R. A. *Ann. Rev. Phys. Chem.* **1964**, *15*, 155−196.
(59) Sumi, H.; Marcus, R. A. *J. Chem. Phys.* **1986**, *84*, 4272−4276.
(60) Jorgensen, W. L.; Madura, J. D.; Swenson, C. J. *J. Am. Chem. Soc.* **1984**, *106*, 6638−6646.
(61) Allen, M. P.; Tildesley, D. J. *Computer Simulation of Liquids*; Oxford: New York, 1987.
(62) Case, D.; Pearlman, D.; Caldwell, J.; Wang, J.; Ross, W.; Simmerling, C.; Darden, T.; Merz, K.; Stanton, R.; Chleng, A.; Vincent, J.; Crowley, M.; Tsui, V.; Gohlke, H.; Radmer, R.; Duan, Y.; Pitera, J.; Massova, I.; Seibel, G.; Singh, U.; Weiner, P.; Kollman, P. *AMBER 7 Users' Manual*; University of California: San Francisco, 2002.
(63) Nose, S. *J. Chem. Phys.* **1984**, *81*, 511.
(64) Hoover, W. G. *Phys. Rev. A* **1984**, *31*, 1695.
(65) Anderson, H. C. *J. Chem. Phys.* **1979**, *72*, 2384−2393.
(66) Smith, W.; Forester, T. R. *The DLPOLY2 User Manual*; Daresbury Laboratory: Daresbury, England, 2001.
(67) Ladanyi, B. M.; Maroncelli, M. *J. Chem. Phys.* **1998**, *109*, 3204−3221.
(68) Kobrak, M. N.; Hammes-Schiffer, S. *J. Phys. Chem. A* **2001**, *105*, 10435−10445.
(69) Ingram, J. A.; Palladino, C. J.; Moog, R. S.; Ito, N.; Biswas, R.; Maroncelli, M. *J. Phys. Chem. B*, submitted for publication.
(70) Karmakar, R.; Samanta, *A. J. Phys. Chem. A* **2002**, *106*, 4447−4452.
(71) Takahashi, S.; Suzuya, K.; Kohara, S.; Koura, N.; Curtiss, L. A.; Saboungi, M.-L. *Z. Phys. Chem.* **1999**, *209*, 209−221.
(72) Elaiwi, A.; Hitchcock, P. B.; Seddon, K. R.; Srinivasan, N.; Tan, Y.-M.; Welton, T.; Zora. J. A. *Dalton Trans.* **1995**, 3467−3472.
(73) Huang, J.-F.; Chen, P.-Y.; Sun, I.-W.; Wang, S. P. *Inorg. Chirm. Acta* **2001**, *320*, 7−11.
(74) Holbrey, J. D.; Seddon, K. R. *J. Chem. Soc., Dalton Trans.* **1999**, *8*, 2133−2139.
(75) Norberg, J.; Nilsson, L. *J. Phys. Chem.* **1995**, *99*, 14876−14884.
(76) Weingärtner, H.; Knocks, A.; Schrader, W.; Kaatze, U. *J. Phys. Chem. A* **2001**, *105*, 8646−8650.
(77) Asaki, M. L. T.; Redondo, A.; Zawodinski, T. A.; Taylor, A. J. *J. Chem. Phys.* **2002**, *116*, 10377−10385.
(78) Hansen, J. P.; McDonald, I. R. *Theory of Simple Liquids*; Academic Press: New York, 1976.
(79) Chandler, D. *Introduction to Modern Statistical Mechanics*; Oxford University Press: New York, 1987.
(80) Tichy, S. E.; Thoen, K. K.; Price, J. M.; Ferra, J. J.; Petucci, C. J.; Kenttamaa, H. I. *J. Org. Chem.* **2001**, *66*, 2726−2733.